

# Chapter 9

## Temperature Dependence of Conductivity in Composite Film of Single-Walled Carbon Nanotubes with Graphene Oxide



Nikita Kurnosov and Victor Karachevtsev

**Abstract** The results of low-temperature studies (5–291 K) of conductivity in the composite film of graphene oxide (GO) with single-walled nanotubes (SWNTs) are presented. The composite film was obtained by vacuum filtration of aqueous suspension containing both GO and SWNTs. It was shown that conductivity of composite is largely conditioned by the nanotubes, while graphene oxide film obtained similarly demonstrated no conductivity. Semiconductor behavior with negative temperature coefficient of conductivity was revealed for both composite and nanotube films. Further analysis confirmed that conductivity in the range of 5–240 K is well described within the framework of the 3D Mott model. The conductivity mechanism involves thermoactivated tunneling of electrons through barriers with a variable range hopping (VRH), which is common for disordered semiconductors. At higher temperatures ( $T > 240$  K) the Arrhenius model was used. Such parameters as distance and energy of electron hopping as well as energy barriers were estimated.

### 9.1 Introduction

Graphene oxide (GO) and single-walled carbon nanotubes (SWNTs) are carbon nanomaterials that exhibit unique physical properties and are promising for applications in such fields as nanoelectronics, photonics, and sensing. GO is graphene with oxygen-containing groups at the edges (carboxyl-COOH and hydroxyl-OH groups) and on the plane (epoxy (C–O–C) and hydroxyl groups) [1, 2]. Due to these groups GO is dispersible in water, which is a major advantage necessary for biomedical purposes [3, 4]. GO sheets contain domains with both  $sp^2$ — and  $sp^3$ —hybridized electrons that govern electronic properties of this nanomaterial. Another important form is reduced graphene oxide (rGO) with partially removed oxygen groups. rGO

---

N. Kurnosov (✉) · V. Karachevtsev  
Department of Molecular Biophysics, B. Verkin ILTPE of NASU, Kharkiv, Ukraine  
e-mail: [n.kurnosov@ilt.kharkov.ua](mailto:n.kurnosov@ilt.kharkov.ua)

V. Karachevtsev  
e-mail: [karachevtsev@ilt.kharkov.ua](mailto:karachevtsev@ilt.kharkov.ua)

© Springer Nature Singapore Pte Ltd. 2020  
A. D. Pogrebnjak and O. Bondar (eds.), *Microstructure and Properties of Micro- and Nanoscale Materials, Films, and Coatings (NAP 2019)*, Springer Proceedings in Physics 240, [https://doi.org/10.1007/978-981-15-1742-6\\_9](https://doi.org/10.1007/978-981-15-1742-6_9)

contains mainly  $sp^2$  domains so that electronic structure is more similar to that of graphene, but it remains soluble in water.

SWNTs have high electrical and thermal conductivity as well as very structure-dependent electronic and optical properties. Significant progress has been made in the production of hybrids formed by carbon nanotubes with rGO or GO [5]. These structures combine 2D GO and 1D SWNTs so that GO sheets are interleaved and connected with nanotubes. At that synergistic effect is possible and resulting characteristics are improved compared to those of individual components. Various methods are proposed to obtain such composites: deposition from suspension under pressure (spray method), vacuum filtration, layer-by-layer deposition, and chemical vapor deposition.

It is expected that GO-SWNTs composite material has a significant potential for use as transparent conductive electrodes in solar cells, active electrodes in supercapacitors or in lithium-ion batteries. The electrical conductivity of GO-SWNTs composites as well as of separate GO/rGO or SWNTs films and networks is a prominent topic of research [6–14]. Mechanism of conductivity can essentially depend on structural peculiarities such as film thickness and alignment of GO or SWNTs and also on the oxidation degree of GO and conductivity type of SWNTs. Variable-range hopping (VRH) [15] and fluctuation-induced tunneling (FIT) [16] conductivity models elaborated for disordered systems are used for approximation of GO-SWNTs and SWNTs conductivity temperature dependence.

The main task of the present work is the study of electronic transport in GO-SWNTs composite film in the temperature range of 5–291 K. The electrical resistance temperature dependence was analyzed using VRH model and also compared with that of SWNTs film. The films were obtained by vacuum filtration method and contained strongly oxidized GO and SWNTs with prevailing content of semiconducting species. The physical characteristics of the films were studied earlier in more detail [17].

## 9.2 Experimental Details

### 9.2.1 Materials

Graphene oxide synthesized by chemical oxidation of graphite using the modified Hummers' method was purchased from Graphenea (San Sebastian, Spain). In GO the content of carbon and oxygen was 49–56% and 41–50%, respectively (so the C/O ratio was 1.2–1.3). The SWNTs grown by chemical vapor deposition CoMoCAT method were purchased from SouthWest NanoTechnologies (USA). The SWNT sample contained predominantly semiconducting nanotubes (~95%), among them, nanotubes of chirality (6, .5) prevailed.

## 9.2.2 Methods

The preparation method of aqueous suspensions of GO-SWNTs hybrids is based on the ultrasound treatment (60 min) of the mixture of the aqueous suspension of GO (mainly monolayers [4]) with carbon nanotubes added to this suspension. The GO concentrations in suspension were  $\sim 0.2$  mg/ml while the weight ratio of GO:SWNT was 1:1. The composite GO-SWNTs films were obtained from aqueous suspensions of GO-SWNTs (0.5–2 ml) deposited on the PTFE membrane (diameter 12.5 mm, pores  $0.24 \mu\text{m}$ , Millipore, USA) by vacuum filtration. The thickness of GO-SWNTs film detached from the membrane was  $\sim 10 \mu\text{m}$ . SWNTs film was prepared similarly from SWNTs suspension in acetone and contained SWNT bundles. The low-temperature measurements of the film conductivity in the range of 5–291 K were carried out in a helium cryostat with temperature stabilization of the film kept in the gas helium atmosphere. The samples were film stripes 0.4–1.5 mm wide attached between contacts distanced at 3 mm, the average rate of temperature changes was about 1.5–2 K/min.

## 9.3 Results and Discussion

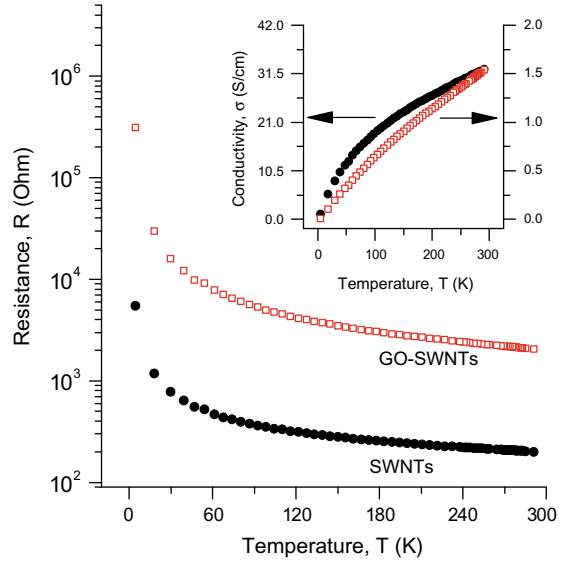
### 9.3.1 Temperature Dependence of GO-SWNTs Composite Film Conductivity

It was found that conductivity of composite GO-SWNTs films depends on the GO:SWNTs ratio. Conductivity was registered for the film with 1:1 ratio and was much smaller or absent at larger ratios. It was concluded that conductivity in obtained composites is largely conditioned by nanotubes, as the pure GO film has shown no conductivity.

The resistance of composite GO-SWNTs film (GO:SWNTs 1:1 ratio) and of SWNTs film was measured in the temperature range of 5–291 K. Data are shown in Fig. 9.1 as well as evaluated conductivities (see Fig. 9.1 inset). Both films demonstrate decrease in conductivity towards low temperatures.

While both films show a negative temperature coefficient of resistance ( $dR/dT < 0$ ), there are certain distinctions in  $\sigma(T)$  behavior. For the GO-SWNTs film conductivity decreased more than 150 times with larger and more uniform slope. So, despite that in composite conductivity occurs mainly through SWNTs, the GO also defines resulting electronic transport. This is because in composite film SWNTs contact not only between themselves but also with GO sheets containing  $sp^2$  and  $sp^3$  domains. Such contacts can create additional energy barriers for electronic transport. Also, most likely, conductive  $sp^2$  domains in strongly oxidized GO sheets do not form continuous network and do not provide conductivity, but still can affect the conductivity of bulk film.

**Fig. 9.1** Temperature dependence of resistance of GO-SWNTs (empty squares) and SWNTs (full circles). Inset shows the specific conductivity of both films (same symbols)



We should specifically note that extrapolation of  $\sigma(T)$  to zero temperature yields zero conductivity for both films studied. Such  $\sigma(T)$  dependence means that most conductive paths contain major disordered areas in which electronic transport is “frozen”. The VRH model proposed by Mott for disordered semiconductors is more appropriate for an approximation of such conductivity temperature dependence [15].

### 9.3.2 Approximation of Temperature Dependencies of GO-SWNTs and SWNTs Films with Different Models

Resistance temperature dependence  $R(T)$  is often considered when experimental data are fitted with certain electronic transport model. This is partially due to the fact that resistance value changes greatly at low temperatures. In the present study we have tested such models as FIT, VRH and Arrhenius equation for approximation of  $R(T)$ .

In the FIT model [16]  $R(T)$  is described as:

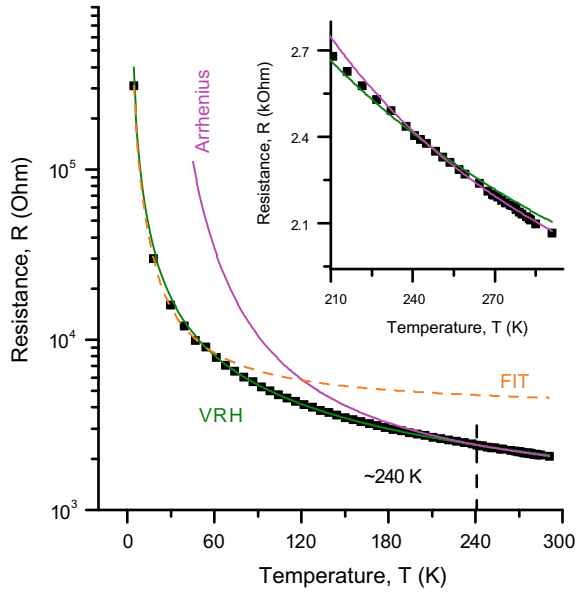
$$R = R_0 \exp[T_1/(T + T_0)], \quad (9.1)$$

where  $R_0$  is a pre-exponential factor,  $T_1$  depends on energy barrier height and width,  $T_0$  is characteristic temperature so that if  $T \ll T_0$  the resistance becomes constant.

In the VRH model [15]  $R(T)$  is described as:

$$R = R_0 \exp\left[\left(T_M/T\right)^{\frac{1}{1+d}}\right], \quad (9.2)$$

**Fig. 9.2** Temperature dependence of GO-SWNTs film resistance fitted with curves according to models described in text. Inset shows high-temperature range where Arrhenius equation is applicable (at  $T > 240$  K)



where  $R_0$  is a pre-exponential factor,  $T_M$  is governed by the density of states in the vicinity of Fermi energy  $N(\epsilon_F)$  and localization length of electron wave function  $\xi$ ,  $d$  depends on the transport dimensionality.

The Arrhenius equation for the  $R(T)$  is as follows:

$$R = R_0 \exp(E_G/k_B T), \tag{9.3}$$

where  $E_G$  is the energy barrier height,  $R_0$  is a pre-exponential factor.

The experimental data for GO-SWNTs film fitted with these three models in different temperature ranges are shown in Fig. 9.2.

It was found that the FIT model (9.1) fits experimental data only in the low-temperature range (5–60 K) and then deviates sharply. In addition, the proper use of FIT model implies that there should be saturation in  $R(T)$  growth below certain temperature  $T_0$ , which was not observed in our experiment (in [11] FIT model was used at temperatures below 2 K). On the contrary, the VRH model (9.2) yields good fit in much wider temperature range, small deviation starts only from 240 K (see Fig. 9.2 inset), where approximation with Arrhenius equation (9.3) is more precise. The results for the SWNTs film were qualitatively similar. On the basis of comparative analysis performed we have chosen VRH (9.2) and Arrhenius (9.3) models for approximation of our experimental data.

Another important stage of approximation was definition of transport dimensionality in VRH model (parameter  $d$  in (9.2)) for our samples. We have considered two values,  $d = 2$  and  $d = 3$  for composite GO-SWNTs, which correspond to two- and

three-dimensional electronic transport. It should be noted that for SWNTs films  $d = 3$  [10, 11] and  $d = 2$  [12] were used earlier at studies of electronic transport.

Experimental data,  $R(T)$ , are plotted in Fig. 9.3 in new coordinates,  $\ln(R)$  and  $T^{-1/(1+d)}$ . It can be derived that (9.2) is transformed into equation of a straight line if such coordinates are used. As it follows from Fig. 9.3, at  $d = 2$  experimental data cannot be fitted linearly, the deviation starts at  $T < 40$  K. On the contrary, at  $d = 3$  linear fit approximates experimental data very well up to  $T \approx 240$  K, and similar results were obtained for SWNTs film. This analysis shows that electronic transport in our samples is effectively three-dimensional and corresponds to 3D VRH model applicable for disordered systems (also called 3D Mott model [15]).

The parameters obtained from the approximation of experimental  $R(T)$  data with VRH and Arrhenius models for GO-SWNTs and SWNTs films are summarized in Table 9.1.

We will briefly discuss parameters obtained from Arrhenius model, while VRH parameters are discussed in the next section. The evaluated energies  $E_G$  yield corresponding temperatures  $T_G = E_G/k_B$  as 212.3 and 130.6 K for GO-SWNTs and SWNTs films respectively. Both  $T_G$  are lower than that temperature range, where Arrhenius model was used, which confirms Arrhenius mechanism as thermal activation of electrons over the energy barriers. We should note that similar energy barriers for rGO (10–50 meV) were reported earlier [7].

**Fig. 9.3** Temperature dependence of GO-SWNTs film resistance in coordinates  $T^{-1/(1+d)}$  and  $\ln(R)$  at  $d = 2$  and  $d = 3$  in VRH model (2)

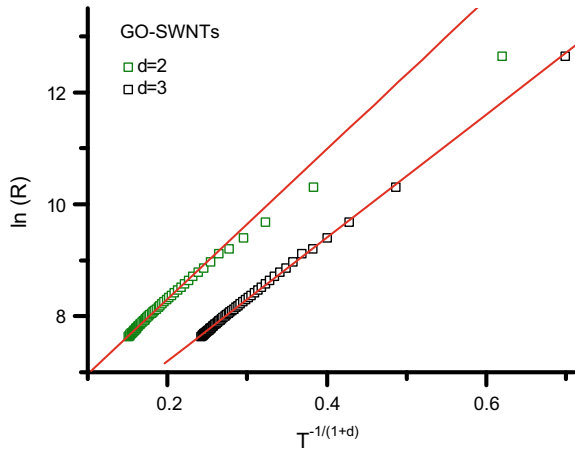


**Table 9.1** The values of parameters obtained in VRH ( $R_0$  and  $T_M$ ) and Arrhenius ( $R_0$  and  $E_G$ ) models for GO-SWNTs and SWNTs films

GO-SWNTs	SWNTs		
VRH	Arrhenius	VRH	Arrhenius
$R_0 = 130.1$ Ohm	$R_0 = 999.4$ Ohm	$R_0 = 34.6$ Ohm	$R_0 = 128.8$ Ohm
$T_M = 17449$ K	$E_G = 18.3$ meV	$T_M = 2857.4$ K	$E_G = 11.3$ meV

### 9.3.3 *Parameters of Electronic Transport in GO-SWNTs and SWNTs Films Within Framework of VRH Model*

VRH model, according to Mott, describes electronic transport that takes place due to tunnelling of electrons between localized states in the potential wells divided by energy barriers [15]. It is also important that additional energy provided by interaction with thermoactivated phonons is needed for tunneling. Probability of tunneling, and consequently conductivity, is defined by the localization length of electron wave function  $\xi$ , electron hopping distance  $r$  and electron hopping energy  $W$ . In this section it is shown that these physical parameters can be derived from fitting parameters obtained from approximation of experimental  $R(T)$  data.

As was mentioned before, parameter  $T_M$  in (9.2) depends on density of states  $N(\varepsilon_F)$  and localization length of electron wave function  $\xi$ . It was shown that in case of 3D VRH ( $d = 3$ ), this relation is [11]:

$$T_M \sim \frac{18.2}{k_B N(\varepsilon_F) \xi^3} \quad (9.4)$$

In order to estimate  $\xi$  for our samples we need to know the density of state value. The analysis of literature data was performed for this task. For example,  $N(\varepsilon_F)$  of two SWNTs samples [11] were evaluated using (9.4) and yielded  $8.5 \times 10^{19}$  and  $7.1 \times 10^{20} \text{ eV}^{-1} \text{ cm}^{-3}$ . As for GO and rGO, data from [18, 19] gives  $N(\varepsilon_F)$  as  $6 \times 10^{18}$  and  $10^{20} \text{ eV}^{-1} \text{ cm}^{-3}$ . Therefore, we can conclude that  $N(\varepsilon_F)$  for different GO and SWNTs samples can vary from  $\sim 10^{19}$  to  $7 \times 10^{20} \text{ eV}^{-1} \text{ cm}^{-3}$ . For the  $\xi$  estimations we have used three  $N(\varepsilon_F)$  values:  $5 \times 10^{20}$ ,  $10^{20}$  and  $10^{19}$ , which yield  $\xi$  as  $\sim 5, 9, 17 \text{ nm}$  for the SWNTs film and  $\sim 3, 5, 11 \text{ nm}$  for the composite GO-SWNTs film. The first two values for our SWNTs sample roughly correlate with data in [11].

Electron hopping distance  $r$  can be defined from  $\xi$  [11]:

$$r = 0.38(T_M/T)^{1/4} \xi \quad (9.5)$$

Note that according to (9.5)  $r$  should increase towards low temperatures. The  $\xi$  and  $r$  (calculated at 5 and 240 K) are presented in Table 9.2.

We can conclude from values in Table 9.2 that  $\xi$  in case of composite GO-SWNTs film is almost twice lower than that of SWNTs film. This, in addition to higher energy barriers (see data from Arrhenius model), partially explains weaker conductivity in GO-SWNTs film. Most likely, SWNTs contacts with GO sheets create additional and more pronounced barriers that decrease  $\xi$  and hamper the electronic transport in composite.

Electron hopping energy was evaluated as [18]:

$$W = \frac{3}{4\pi N(\varepsilon_F) r^3} \quad (9.6)$$

**Table 9.2** The estimated values of localization length  $\xi$  and hopping distance  $r$  obtained in VRH model at different densities of states  $N(\epsilon_F)$  for GO-SWNTs and SWNTs films

Sample	$N(\epsilon_F)$ ( $\text{eV}^{-1} \text{ cm}^{-3}$ )	$\xi$ (nm)	$r$ at 5 K (nm)	$r$ at 240 K (nm)
SWNTs	$5 \times 10^{20}$	5.4	9.9	3.6
	$10^{20}$	9.2	16.9	6.2
	$10^{19}$	17	34.7	12.7
GO-SWNTs	$5 \times 10^{20}$	2.9	8.4	3.1
	$10^{20}$	5	14.5	5.3
	$10^{19}$	10.7	31.1	11.4

As the  $r$  increases at low temperature,  $W$  should decrease which is a consequence of smaller energy of thermoactivated phonons. Decreased  $W$  is a reason which makes necessary longer-range tunneling at low temperatures and results in decreased conductivity.

We have plotted the hopping range and hopping energy temperature dependencies for both GO-SWNTs and SWNTs films (using the density of states value  $N(\epsilon_F) = 10^{20} \text{ eV}^{-1} \text{ cm}^{-3}$  which gave rather good correlation of calculated  $\xi$  with literature data).  $r(T)$  and  $W(T)$  are presented in Fig. 9.4a and b respectively. It can be seen that in the whole temperature range of 5–240 K  $r$  is lower for GO-SWNTs film. The situation is opposite for  $W$ . We have noted that at 240 K the value of hopping energy  $W$  reached 9 and 14 meV for the SWNTs and GO-SWNTs films respectively, which is only slightly lower energy barriers height evaluated from Arrhenius model (11 and 18 meV). This means that roughly near 240 K VRH tunneling transport mechanism is gradually changed to over-the-barrier electron activation described by Arrhenius equation.

We should also note that for the SWNTs film the condition  $W(T) < k_B T$  is fulfilled in the whole temperature range. This is also the case for GO-SWNTs film, except for the range 5–60 K in which  $W(T) \approx k_B T$ . This observation implies the viability of VRH model as the hopping energy should be of the same value order or less than thermal energy. The  $W(T)$  dependencies calculated using other  $N(\epsilon_F)$  values, namely,  $5 \times 10^{20}$  and  $10^{19} \text{ eV}^{-1} \text{ cm}^{-3}$ , have shown that for our samples the  $N(\epsilon_F)$  most likely lies in the interval  $10^{20} - 5 \times 10^{20} \text{ eV}^{-1} \text{ cm}^{-3}$ .

## 9.4 Conclusions

The analysis of resistance of composite film GO-SWNTs (components ratio 1:1) containing strongly oxidized graphene oxide and nanotubes with prevailing content of semiconducting species was performed in the temperature range of 5–291 K. It was shown that conductivity of composite film is due to nanotubes present, as the GO film had no conductivity and SWNTs film displayed rather large conductivity. The



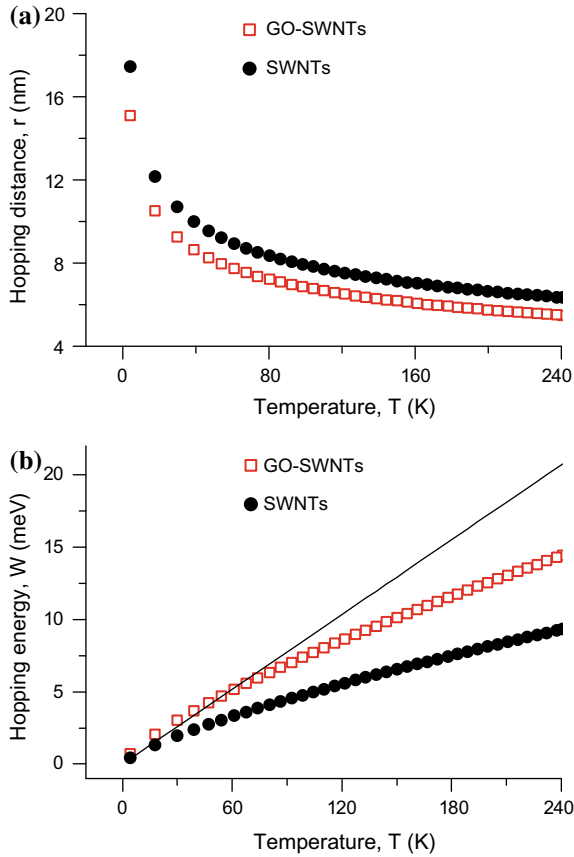


**Fig. 9.4** Temperature dependencies of hopping distance  $r$  (a) and hopping energy (b) calculated for the GO-SWNTs (empty squares) and SWNTs (full circles) films. The straight line in Fig. 9.4b denotes the thermal energy  $k_b T$

decrease of conductivity towards low temperature is similar to conductivity behavior in disordered semiconductor systems.

Three-dimensional variable-range hopping model of electronic transport (3D Mott model) based on tunneling of electrons between localized states near Fermi energy was proved applicable for the resistance of both GO-SWNTs and SWNTs films in the low-temperature range of 5–240 K. The Arrhenius model was used for the higher temperatures ( $T > 240$  K). Approximation of experimental data using these models resulted in evaluation of such parameters of electron transport as localization length  $\xi$ , hopping distance  $r$ , hopping energy  $W$  and energy barriers  $E_G$ . The density of states near Fermi energy  $N(\epsilon_F)$  was estimated to be in the interval  $10^{20} - 5 \times 10^{20} \text{ eV}^{-1} \text{ cm}^{-3}$ .

It was shown that at temperature increase from 5 to 240 K hopping distance  $r$  is decreased in three times for both GO-SWNTs and SWNTs films. The comparison of

$r(T)$  and  $W(T)$  between GO-SWNTs and SWNTs film showed that hopping distance  $r$  is larger for the SWNTs film, while situation is opposite for hopping energy  $W$ . Also, in case of GO-SWNTs film localization length  $\xi$  is twice lower comparing to SWNTs film while energy barrier  $E_G$  is higher. This implies that additional contacts between GO surface and nanotubes hamper the resulting electronic transport.

**Acknowledgements** Authors thank A.M. Plokhotnichenko and A.S. Linnik for the help provided in low-temperature experiments. This work was partially supported by funding from the National Academy of Sciences of Ukraine (NASU) (Grant N 15/19-H, Grant N 07-01-18/19). N.K. acknowledges support from the NASU Grant 1/H-2019.

## References

1. C.K. Chua, M. Pumera, Chemical reduction of graphene oxide: a synthetic chemistry viewpoint. *Chem. Soc. Rev.* **43**, 291–312 (2014). <https://doi.org/10.1039/C3CS60303B>
2. R.K. Singh, R. Kumar, D.P. Singh, Graphene oxide: strategies for synthesis, reduction and frontier applications. *RCS Adv.* **6**, 64993–65011 (2016). <https://doi.org/10.1039/C6RA07626B>
3. S.S. Nanda, G.C. Papaefthymiou, D.K. Yi, Functionalization of graphene oxide and its biomedical applications. *Crit. Rev. Solid State Mater. Sci.* **40**, 291–315 (2015). <https://doi.org/10.1080/10408436.2014.1002604>
4. M.V. Karachevtsev, S.G. Stepanian, AYu. Ivanov, V.S. Leontiev, V.A. Valeev, O.S. Lytvyn, L. Adamowicz, V.A. Karachevtsev, Binding of polycydylic acid to graphene oxide: spectroscopic study and computer modeling. *J. Phys. Chem. C* **121**, 18221–18233 (2017). <https://doi.org/10.1021/acs.jpcc.7b04806>
5. H.X. Kong, Hybrids of carbon nanotubes and graphene/graphene oxide. *Curr. Opin. Solid State Mater. Sci.* **17**, 31–37 (2013). <https://doi.org/10.1016/j.cossms.2012.12.002>
6. Q. Zheng, B. Zhang, X. Lin, X. Shen, N. Yousefi, Z.-D. Huang, Z. Li, J.-K. Kim, Highly transparent and conducting ultralarge graphene oxide/single-walled carbon nanotube hybrid films produced by Langmuir-Blodgett assembly. *J. Mater. Chem.* **22**, 25072–25082 (2012). <https://doi.org/10.1039/C2JM34870E>
7. V. Skakalova, A.B. Kaiser, Y.-S. Woo, S. Roth, Electronic transport in carbon nanotubes: From individual nanotubes to thin and thick networks. *Phys. Rev. B* **74**, 085403–1–10 (2006). <https://doi.org/10.1103/physrevb.74.085403>
8. G. Eda, C. Mattevi, H. Yamaguchi, H. Kim, M. Chhowalla, Insulator to semimetal transition in graphene oxide. *J. Phys. Chem. C* **113**, 15768–15771 (2009). <https://doi.org/10.1021/jp9051402>
9. V. Skakalova, V. Vretenar, L. Kopera, P. Kotrusz, C. Mangler, M. Mesko, J.C. Meyer, M. Hulman, Electronic transport in composites of graphite oxide with carbon nanotubes. *Carbon* **72**, 224–232 (2014). <https://doi.org/10.1016/j.carbon.2014.02.006>
10. C. Morgan, Z. Alemipour, M. Baxendale, Variable range hopping in oxygen-exposed single-wall carbon nanotube networks. *Phys. Stat. Sol. A* **205**, 1394–1398 (2008). <https://doi.org/10.1002/pssa.200778113>
11. M. Salvato, M. Lucci, I. Ottaviani, M. Cirillo, S. Orlanducci, E. Tamburri, V. Guglielmotti, F. Toschi, M.L. Terranova, M. Pasquali, Low temperature conductivity of carbon nanotube aggregates. *J. Phys.: Condens. Matter* **23**, 475302–1–7 (2011). <https://doi.org/10.1088/0953-8984/23/47/475302>
12. S. Ravi, A.B. Kaiser, C. Bumby, Charge transport in surfactant-free single walled carbon nanotube networks. *Phys. Stat. Sol. B* **250**, 1463–1467 (2013). <https://doi.org/10.1002/pssb.201300033>

13. H.-J. Kim, D. Kim, S. Jung, S.N. Yi, Y.J. Yun, S.K. Chang, D.H. Ha, Charge transport in thick reduced graphene oxide film. *J. Phys. Chem. C* **119**, 28685–28690 (2015). <https://doi.org/10.1021/acs.jpcc.5b10734>
14. R. Cheruku, D.S. Bhaskaram, G. Govindaraj, Variable range hopping and relaxation mechanism in graphene oxide sheets containing sp<sup>3</sup> hybridization induced localization. *J. Mater. Sci.: Mater. Electron.* **29**, 9663–9673 (2018)
15. N.F. Mott, E.A. Davis, *Electronic Processes in Non-Crystalline Materials* (Clarendon, Oxford, 1979), pp. 1–608
16. P. Sheng, Fluctuation-induced tunneling conduction in disordered materials. *Phys. Rev. B* **21**, 2180–2195 (1980). <https://doi.org/10.1103/PhysRevB.21.2180>
17. V.A. Karachevtsev, A.M. Plokhotnichenko, M.V. Karachevtsev, A.S. Linnik, N.V. Kurnosov, Composite films of single-walled carbon nanotubes with strong oxidized graphene: characterization with spectroscopy, microscopy, conductivity measurements (5–291 K) and computer modeling. *Low Temp. Phys.* **45**(7), 881–891 (2019). <https://doi.org/10.1063/1.5111303>
18. B. Muchharla, T.N. Narayanan, K. Balakrishnan, P.M. Ajayan, S. Talapatra, Temperature dependent electrical transport of disordered reduced graphene oxide. *2D Materials* **1**, 011008-1–011008-10 (2014). <https://doi.org/10.1088/2053-1583/1/1/011008>
19. R. Kumar, A. Kaur, I.E.T. Circ, *Device Syst.* **9**, 392 (2015)